

UC Irvine

UC Irvine Previously Published Works

Title

Ceftriaxone inhibits stress-induced bladder hyperalgesia and alters cerebral micturition and nociceptive circuits in the rat: A multidisciplinary approach to the study of urologic chronic pelvic pain syndrome research network study

Permalink

<https://escholarship.org/uc/item/2ns0t9t4>

Journal

Neurourology and Urodynamics, 39(6)

ISSN

0733-2467

Authors

Holschneider, Daniel P
Wang, Zhuo
Chang, Huiyi
et al.

Publication Date

2020-08-01

DOI

10.1002/nau.24424

Peer reviewed



Published in final edited form as:

NeuroUrol Urodyn. 2020 August ; 39(6): 1628–1643. doi:10.1002/nau.24424.

Ceftriaxone inhibits stress-induced bladder hyperalgesia and alters cerebral micturition and nociceptive circuits in the rat: A multidisciplinary approach to the study of urologic chronic pelvic pain syndrome (MAPP) research network study

DP Holschneider^{a,*}, Z Wang^a, HH Chang^{b,+}, R Zhang^b, Y Gao^{b,#}, Y Guo^a, J Mao^b, LV Rodriguez^{b,*}

^aDepartment of Psychiatry and Behavioral Sciences, University of Southern California, Los Angeles, California, United States of America

^bDepartment of Psychiatry Urology at University of Southern California, Los Angeles, California, United States of America

Abstract

Aims—Emotional stress plays a role in the exacerbation and development of interstitial cystitis/bladder pain syndrome (IC/BPS). Given the significant overlap of brain circuits involved in stress, anxiety, and micturition, and the documented role of glutamate in their regulation, we examined the effects of an increase in glutamate transport on central amplification of stress-induced bladder hyperalgesia, a core feature of IC/BPS.

Methods—Wistar-Kyoto rats were exposed to water avoidance stress (WAS, 1 hour/day × 10 days) or sham stress, with subgroups receiving daily administration of ceftriaxone (CTX), an activator of glutamate transport. Thereafter, cystometrograms were obtained during bladder infusion with visceromotor responses (VMR) recorded simultaneously. Cerebral blood flow (CBF) mapping was performed by intravenous injection of [¹⁴C]-iodoantipyrine during passive bladder distension. Regional CBF was quantified in autoradiographs of brain slices and analyzed in 3D reconstructed brains with statistical parametric mapping.

Results—WAS elicited visceral hypersensitivity during bladder filling as demonstrated by a decreased pressure threshold and VMR threshold triggering the voiding phase. Brain maps revealed stress effects in regions noted to be responsive to bladder filling. CTX diminished visceral hypersensitivity and attenuated many stress-related cerebral activations within the supraspinal micturition circuit and in overlapping limbic and nociceptive regions, including the posterior midline cortex (posterior cingulate/anterior retrosplenium), somatosensory cortex, and anterior thalamus.

*Corresponding authors: lrodriguez@med.usc.edu, holschne@usc.edu, University of Southern California, Keck School of Medicine, Los Angeles, CA 90033.

⁺Current address: Urology and Reeve-Irvine Research Center, University of California Irvine, 837 Health Science Road, Gillespie 2111, Zot Code 4265, Irvine, CA 92697

[#]Current address: Department of Urology, the Second Xiangya Hospital, Central South University, Changsha, Hunan, China

Conclusions—CTX diminished bladder hypersensitivity and attenuated regions of the brain that contribute to nociceptive and micturition circuits, show stress effects, and have been reported to demonstrated altered functionality in IC/BPS patients. Glutamatergic pharmacologic strategies modulating stress-related bladder dysfunction may be a novel approach to the treatment of IC/BPS.

Keywords

water avoidance stress; painful bladder syndrome/interstitial cystitis; animal model; brain mapping; micturition; glutamate

1. Introduction

Interstitial cystitis/bladder pain syndrome (IC/BPS) is a chronic bladder pain disorder associated with urinary frequency affecting up to 7 million women per year. The majority of these patients report pain beyond the pelvis and 38% experience widespread pain.¹ Its pathophysiology is poorly understood and current treatments are ineffective. Physical and emotional stress plays a role in the exacerbation, and possibly in the development of IC/BPS.^{2–7} Recently, a large multisite research network study (multidisciplinary approach to the study of urologic chronic pelvic pain syndrome, MAPP) has demonstrated that IC/BPS patients have multiple psychosocial difficulties and high levels of lifetime/current stress when compared to controls, and stress correlates to worsening of symptoms.^{5, 8} This has led to a disease conceptualization in which IC/BPS and other often coexisting functional pain disorders can be viewed as a cluster of biological endophenotypes which appear to be stress sensitive^{6, 9–13}, with a possible abnormality in sensory gating.^{14, 15} Consistent with this, the MAPP research network has recently identified potential central biological markers for IC/BPS, which include functional alterations in a sensorimotor network, abnormal connectivity of posterior medial cortex, and brain microstructural changes associated with chronic pain, bladder function, and symptom severity.^{16–24}

Our prior work^{25–29} has employed a reverse translational rodent model that parallels the clinical phenotype of IC/BPS, in particular the role of chronic stress in the development and maintenance of urinary symptoms and bladder hypersensitivity,^{2, 30–34} as well as general pain sensitivity in susceptible individuals predisposed to anxiety.^{8, 35–39} In this model, we have demonstrated that chronic water avoidance stress (WAS) leads to urinary frequency, bladder hyperalgesia, and increased somatosensory nociceptive reflex responses that persist up to 1 month following removal of the stressor. In addition, WAS rats compared to control animals show a heightened activation of the posterior cingulate/anterior retrosplenial cortex to bladder distension²⁹, a brain region previously demonstrated to show altered functional brain connectivity in a cohort of patients with urologic chronic pelvic pain syndrome (UCPPS).¹⁹

There is overwhelming preclinical evidence that modulation of glutamate alters pain thresholds.^{25, 40–43} Clinically, a number of chronic pain syndromes demonstrate increases in glutamate in brain regions associated with pain and stress modulation.^{44–49} GLT-1 (human homologue EAAT-2) is the quantitatively dominant glutamate transporter in mammals and is

mainly expressed by astrocytes. Decreased expression of glial GLT-1 in areas of the brain and spinal cord following stress is hypothesized to be a major factor influencing chronic pain, as well as mood disorders, depression, and other psychiatric conditions.^{40, 50–54} Recent data suggests that enhanced glutamate uptake reduces visceral pain responses, both in GLT-1 overexpressing mice and following administration of ceftriaxone or riluzole, activators of GLT-1.^{41, 55–57} In fact, glutamate neurotransmission has been shown to play a role in the pathophysiology of bladder hyperalgesia in the WAS model of IC/BPS.²⁵ In this model, stress induced bladder hyperalgesia and increased urinary frequency correlated with decreases in spinal GLT-1 expression. Similarly, administration of dihydrokainate, an inhibitor of the GLT-1 transporter, resulted in visceral hyperalgesia. In contrast, when GLT-1 expression was increased via administration of intraperitoneal ceftriaxone, there was an attenuation of pre-existing pain and voiding dysfunction. Based on these findings, the current study examined the effects of glutamate modulation by CTX administration during WAS exposure on the subsequent development of stress-induced bladder hyperalgesia and its effects on micturition and nociceptive circuits.

2. Methods

2.1. Animals

Adult, female Wistar-Kyoto (WKY) rats (strain 008, Charles River, Wilmington, MA, USA), a high anxiety strain predisposed to stress were studied.^{25, 27, 58} Rats were housed in groups of two under standard vivaria conditions (lights on from 7 a.m. to 7 p.m.), with direct bedding, and with ad libitum access to food (Laboratory Rodent Diet 5001, Constant Nutrition) and water (internal reverse osmosis system). Female rats were the primary focus as the prevalence of IC/BPS is greatest in women.⁵⁹ Experimental procedures were conducted in accordance with the National Research Council Guide for the Care and Use of Laboratory Animals and were approved by the Institutional Animal Care and Use Committee of the University of Southern California.⁶⁰

2.2. Water avoidance stress

Methods have been previously published in detail.^{25, 29} WAS involved placing the rats for 1 hr./day over 10 days on a pedestal in a water-filled tank.^{58, 61, 62} Controls included sham animals exposed to handling only and kept in its home cage in the experimental room for 1 hr./day. One hour prior to being exposed to WAS or the control condition (WAS-CTX, n=10, 13.6 ± 0.5 weeks; SHAM-CTX, n=10, 13.4 ± 0.5 weeks), animals received CTX, a β -lactam antibiotic that increases GLT-1 expression (Sigma-Aldrich, St. Louis, MO, 200 mg/kg, i.p. in a volume of 333 mg/ml). The dose of CTX was based on our prior work.²⁵ Comparison was made to animals that did not receive CTX (WAS, n=7, 12.3 ± 0.4 weeks; SHAM, n=7, 13.3 ± 0.4 weeks). All results of CTX treatment were compared to previously published results of WAS vs. SHAM groups.²⁹

2.3. Surgical procedures

One day after completion of the WAS protocol and final administration of CTX, rats received placement of an external jugular vein catheter under isoflurane anesthesia (1.5–2%). Forty mg/mL of α -chloralose (Sigma Aldrich, St. Louis, MO, USA) was dissolved in

20% β -cyclodextrin (Sigma Aldrich, St. Louis, MO, USA) and administered intravascularly as a bolus (40 mg/kg). We chose light sedation using α -chloralose because of its favorable profile in maintaining cerebral function intact⁶³ as compared to isoflurane^{64, 65} or urethane.⁶⁶ Isoflurane anesthesia was maintained at 1% for 30 minutes to allow the α -chloralose to take effect. Two fine and insulated silver wire electrodes (0.05 mm diameter, A-M Systems, Everett, WA, USA) with exposed tips were embedded into the left abdominal external oblique muscle for recording of the visceromotor response (VMR, 1kHz sampling rate). A PE-50 catheter was inserted into the bladder through the urethra. The bladder catheter was connected to an infusion pump (KD Scientific) and a pressure sensor (MP150, Biopac Systems Inc., Goleta, CA, USA) via a 3-way connector.

2.4. Measurement of CMG and VMR recordings

After completion of the surgical procedures, the animals were maintained under conscious sedation with α -chloralose infusion (15 mg/kg/hr, i.v.). Recordings were begun 1 hour after discontinuation of isoflurane anesthesia. To obtain the cystometrogram (CMG), the bladder was continuously infused with room temperature normal saline (0.9%, 0.1 mL/min) via the urethral catheter and attached pressure sensor, with the animal allowed to void spontaneously per urethra around the catheter. Data were recorded by a data acquisition system (MP150, Biopac Systems Inc., Goleta, CA, USA) and analyzed using AcqKnowledge® 4.1 (Biopac Systems Inc., Goleta, CA, USA). Three consecutive voiding cycles were recorded and the following parameters were obtained: latency to void or leak (LV), maximum intravesical pressure (IVP_{max}), and pressure threshold to void or leak (PT). PT was defined as the intravesical pressure before a reflex voiding contraction or the pressure prior to a leak as previously described and illustrated in the WAS animal model.²⁶ Bladder capacity was calculated from the first void (bladder empty) to the next void as latency \times infusion rate (0.1mL/min). The pressure in the bladder that evoked a VMR response (VMR threshold, cmH₂O) was recorded for each animal, and the normalized ratio of VMR threshold/IVP_{max} was calculated. Data was expressed as means (\pm standard errors). A non-parametric Mann-Whitney test was used for the between group analysis (P<0.05) using GraphPad Prism 7 (GraphPad Software Inc., LaJolla, CA, USA).

2.5. Functional Brain Mapping

After completion of the CMG, intrabladder distension was performed. The urethra was occluded with a 5-0 silk suture and the animal was allowed to accommodate for 30 minutes. Using a saline-filled reservoir, the bladder was distended to a pressure of 20cmH₂O. [¹⁴C]-iodoantipyrine (100 μ Ci/kg, American Radiolabelled Chemicals, Inc., St. Louis, MO, USA) was bolus infused at 45 seconds following bladder distension and in the absence of a VMR response. Radiotracer administration was immediately followed by infusion of a euthanasia solution (pentobarbital 50 mg/mL, 3M KCl), which resulted in cardiac arrest within 10s, a rapid fall of arterial blood pressure, termination of brain perfusion, and death.⁶⁷ This 10s time window provided the temporal resolution during which the distribution of rCBF-related tissue radioactivity was mapped.

2.5.1. Autoradiography—Brains were flash frozen and serially sectioned (60 coronal 20- μ m slices, 300- μ m interslice distance). Autoradiographic images along with [¹⁴C]

standards (Amersham Biosci.) were digitized and CBF-related tissue radioactivity was measured.^{68–70} The [14C]- iodoantipyrine method has an estimated spatial resolution of 100 μm .⁷¹

2.5.2. Statistical Parametric Mapping—3-D brains were reconstructed and spatially normalized to a template, then analyzed using statistical parametric mapping (SPM-5)⁷² as per our prior methods.⁷³ Changes in rCBF were analyzed with voxel-wise factorial analysis and t-tests ($P < 0.05$, with > 100 contiguous voxels considered statistically significant).⁷³ We first ran a factorial analysis, equivalent to running an analysis of variance (ANOVA) test at each voxel, to identify rCBF changes reflecting main effects of “Stress”, “Ceftriaxone”, and “Stress \times Ceftriaxone” interaction. To further delineate direction of those rCBF changes, we performed between-group Student’s t-test (two-tailed). Brain regions were identified using coronal, sagittal and transverse views according to the rat brain atlas.⁷⁴

2.5.3. Seed correlation analysis—Because of the broad and significant stress-related group difference noted in our analysis in the posterior cingulate/anterior retrosplenial cortex (pCg/antRS), as well as the potential role of this region as a central biological markers for IC/BPS²⁹, the right pCg/antRS was used in a seed correlation analysis. An ROI was manually drawn on the template brain, with definition of the pCg/antRS as defined by the rat brain atlas.⁷⁴ A functional ROI was created by combining anatomically defined ROIs with the significant SPM clusters through logical conjunction as previously described.⁷⁵ Mean optical density of each functional ROI was extracted for each animal using the Marsbar toolbox for SPM (version 0.42, <http://marsbar.sourceforge.net/>). Seed correlation was analyzed in SPM across the whole brain, with color-coded correlation coefficients ($P < 0.05$, extent threshold > 100 significant, contiguous voxels).

3. Results

3.1. CMG and VMR recordings

Results of the WAS vs. SHAM comparison have been previously published²⁹. In summary, these showed that WAS animals compared to controls demonstrated a decreased pressure threshold (PT) and VMR threshold triggering the voiding phase. VMR evoked by bladder distension in WAS animals appeared at a lower IVP during bladder filling compared to SHAM. The percentage of VMR threshold pressure/maximum intravesical pressure (IVPmax) also showed the VMR appeared earlier in WAS animals compared to SHAM. All these are surrogates for bladder hypersensitivity. The maximum IVP and bladder capacity showed no significant changes between SHAM and WAS groups. In the current study, administration of CTX did not result in significant changes in maximum voiding pressure (Fig. 1A) and PT of WAS-CTX or SHAM-CTX animals, though WAS-CTX animals showed a trend toward restoration of PT to levels noted in SHAM-CTX (Fig. 1B). CTX restored the appearance of VMR towards that of SHAM as measured by VMR thresholds (Fig. 1C, $p = 0.04$) and the percentage of VMR threshold/IVPmax (Fig. 1D, $p = 0.006$) suggesting improvements in overall bladder hypersensitivity.

3.2. Functional brain mapping

3.2.1. Effect of stress—Analysis of variance (ANOVA) revealed significant main effects of ‘Stress’ ($P < 0.05$, >100 contiguous voxels) as summarized in Table 1. Main effects were bilateral, except as noted otherwise. Within the micturition circuit, this included the anterior-most cingulate and posterior cingulate/anterior retrosplenial (pCg/antRS) cortices, posterior insular cortex, hypothalamus (anterior, posterior, ventromedial), thalamus (anterior medial, anterior ventral, lateral dorsal, mediodorsal, paraventricular nuclei), dorsal hippocampus, amygdala (medial, basomedial, cortical), periaqueductal gray, as well as less broadly in the medial prefrontal (prelimbic, orbital, anterior dorsal cingulate) and in secondary motor cortices. Outside the micturition circuit, a significant main effect of ‘Stress’ was noted in somatosensory cortex (primary, secondary), and significantly, though less broadly, in the posterior piriform and visual (primary, secondary) cortices, as well as in anterior, ventral striatum and the simple cerebellar lobule.

T-tests (Figs. 2, 3) revealed that WAS compared to SHAM rats showed a significantly greater regional cerebral blood flow (rCBF, $P < 0.05$, >100 contiguous voxels) in regions of the micturition circuit, including the pCg/antRS, posterior insula, the hypothalamus (anterior, ventromedial), nuclei of the thalamus associated with limbic modulation (anterior medial, anterior ventral, lateral dorsal, mediodorsal, paraventricular nuclei), and significantly, though less broadly, in medial prefrontal (prelimbic, orbital), secondary motor cortices, and the parabrachial/Barrington nuclear complex. Significant decreases in rCBF were noted in the dorsal posterior hippocampus, amygdala (basomedial, cortical, medial), and posterior hypothalamus. Outside the micturition circuit, WAS compared to SHAM rats showed a significantly greater rCBF ($P < 0.05$, >100 contiguous voxels) in the somatosensory (primary, secondary), piriform, entorhinal and visual (primary, secondary) cortices, dorsomedial striatum, raphe and superior colliculus.²⁹ Significant decreases in rCBF were noted in the anterior ventral striatum, and cerebellar simple lobule.

3.2.2. Effect of CTX—ANOVA revealed also a significant main effect of ‘Ceftriaxone’ ($P < 0.05$, >100 contiguous voxels) as summarized in Table 1. In the micturition circuit, this included the dorsal midline cortex (prelimbic prefrontal, anterior-to-mid cingulate, mid-to-posterior retrosplenial), entorhinal, primary and secondary motor cortices, posterior insula, dorsal hippocampus (anterior, posterior), amygdalar nuclei (basolateral, basomedial, central, cortical, lateral, medial), hypothalamus (anterior, preoptic area, ventromedial), thalamic nuclei (anterior medial, anterior ventral, medial geniculate, mediodorsal, paraventricular, ventroposterior lateral, ventroposterior medial, ventrolateral, ventromedial), periaqueductal gray, periventricular gray, and parabrachial/Barrington’s nuclear complex. Outside the micturition circuit, a significant main effect of ‘Ceftriaxone’ was also noted in somatosensory cortex (primary, secondary), olfactory, piriform and visual cortex (primary, secondary), as well as the striatum (dorsal, dorsomedial, lateral, ventral), ventral pallidum, nucleus accumbens, lateral septum, diagonal band, linear raphe, postsubiculum, deep mesencephalic/tegmental area, retrorubral field, pons, inferior colliculus, superior olive, vermis and simple cerebellar lobule.

In the ANOVA, the main effects of ‘Stress’ and of ‘Ceftriaxone’ were significant in several shared brain regions within the micturition circuit, including in midline cortex (prelimbic prefrontal, anterior cingulate, posterior cingulate), insula and motor (secondary) cortices, thalamus (anterior medial, anterior ventral, mediodorsal, paraventricular nuclei), and dorsal anterior hippocampus, amygdala (basomedial, cortical, medial), hypothalamus (anterior, ventromedial), periaqueductal gray, periventricular gray, as well as in the somatosensory cortex (primary, secondary). In these regions, the magnitude of the ‘Ceftriaxone’ effect typically exceeded that of the ‘Stress’ effect (Table 1).

T-tests showed the effect of CTX to have a near identical distribution in both the WAS, as well as the SHAM animals (Fig. 2). Within the micturition circuit (Fig. 3), both the WAS-CTX vs. WAS and for the SHAM-CTX vs. SHAM comparisons demonstrated a significant ($P < 0.05$, >100 contiguous voxels) increase in rCBF in midline cortex (prelimbic prefrontal, anterior-to-mid dorsal cingulate), motor cortex (primary, secondary), anterior dorsal hippocampus, periventricular gray, and periaqueductal gray, with significant decreases in rCBF in posterior insula, amygdala (basolateral, basomedial, lateral, medial), sensory nuclei of the thalamus (posterior, ventroposterior lateral/ventroposterior medial nuclei), anterior hypothalamus, and the parabrachial/Barrington’s nuclear complex. Outside the micturition circuit, a significant increase in rCBF was noted in response to CTX for both WAS and SHAM rats in primary somatosensory cortex (hindlimb, trunk area), visual cortex (primary, secondary), deep mesencephalic/tegmental area, lateral septum, retrorubral field, raphe, vermis and cerebellar simple lobule. A significant decrease in rCBF ($P < 0.05$, >100 contiguous voxels) was noted in primary somatosensory cortex (upper lip; barrel field area), secondary somatosensory cortex, olfactory, and piriform cortices, superior olive, striatum (dorsal, dorsomedial, lateral, ventral), nucleus accumbens, ventral pallidum, and inferior colliculus. Differences in the WAS-CTX vs. WAS and the SHAM-CTX vs. SHAM comparison were noted in the pCg/antRS, where there was a relative decrease in rCBF in WAS-CTX vs. WAS and a relative increase in the SHAM-CTX vs. SHAM comparison. Differences in the WAS-CTX versus SHAM-CTX comparison were limited, with small significant increases in rCBF in the anterior cingulate, orbital prefrontal cortex, primary somatosensory cortex, and the amygdala (basomedial, medial).

3.2.3. Stress × ceftriaxone interaction—A significant interaction of ‘Stress × Ceftriaxone’ (ANOVA, $P < 0.05$, >100 contiguous voxels) was noted in pCg/antRS and to a lesser extent in the primary somatosensory (trunk area, S1Tr), secondary somatosensory and entorhinal cortices. Subcortically, a significant ‘Stress × Ceftriaxone’ interaction was noted in the amygdala (basomedial, medial nuclei), thalamus (anteromedial, anteroventral, lateral dorsal nuclei), hypothalamus (posterior, ventromedial), and simple cerebellar lobule (Table 1).

3.2.4. Stress effect on functional connectivity of the posterior cingulate/ anterior retrosplenial cortex—Because of the broad and significant stress-related group difference noted in our analysis in the pCg/antRS, as well as the potential role of this region as a central biological markers for UCPPS^{19, 29}, the right pCg/antRS was used in a seed correlation analysis (Fig. 4). The right pCg/antRS cortex in WAS rats showed significant

bilateral positive functional connectivity ($P < 0.5$, >100 contiguous voxels) across regions of the micturition circuit, including midline cortex (prelimbic, anterior cingulate), posterior motor cortex (primary, secondary), mid to posterior insular cortex, the anterior hypothalamus, thalamus (anteromedial, anteroventral, ventral lateral), anterior dorsal hippocampus, anterior amygdala (basolateral, basomedial, central, lateral, medial nuclei), and the parabrachial/Barrington nucleus complex. In addition, significant bilateral positive functional connectivity was demonstrated with orbital cortex, somatosensory cortex (primary, secondary), visual cortex (primary, secondary), as well as the right postsubiculum, lateral septal nucleus, striatum (posterior dorsomedial, posterior lateral), and posterior superior colliculus.

Significant negative functional connectivity ($P < 0.05$, > 100 contiguous voxels) of the pCg/antRS of WAS animals was noted with bilateral posterior hippocampus, hypothalamus (ventromedial, lateral), the thalamus (lateral dorsal, lateral posterior, mediodorsal, posterior, ventromedial, ventral posterolateral, ventral posteromedial, midline/intralaminar nuclei), posterior amygdala (basolateral, basomedial, central, lateral, medial nuclei), periaqueductal gray, periventricular gray, as well as with ectorhinal/perirhinal cortex, anterior-most ventral striatum, and the nucleus accumbens.

Compared to SHAM rats, WAS rats showed broader and more numerous regions of significant positive functional connectivity to the right pCg/antRS cortex ($P < 0.05$, >100 contiguous voxels). Within the micturition circuit, several of the regions that were significant in both WAS and SHAM rats, had substantially larger cluster sizes in WAS than in the SHAM animals. This included a broader significant positive functional connectivity with the posterior insula and anterior thalamus, and a broader significant negative functional connectivity with the posterior thalamus (mediodorsal, posterior, ventromedial, ventral posteromedial, lateral posterior, and midline/intralaminar nuclei) and periventricular gray/ anterior periaqueductal gray region. In addition, a spatially broader and significant positive functional connectivity was noted with somatosensory cortex (primary, secondary), and visual cortex (primary, secondary), as well as postsubiculum.

3.2.5. Ceftriaxone effect on functional connectivity of the posterior cingulate/ anterior retrosplenial cortex—Prior administration of CTX diminished or reversed the positive functional connectivity of the pCg/antRS. Thus, WAS-CTX animals showed a significant bilateral negative functional connectivity with the midline cortex (prelimbic, anterior-to-mid dorsal cingulate), motor cortex (primary, secondary), posterior insular cortex, as well as orbital cortex, and somatosensory cortex (primary, secondary) – opposite to the findings in the WAS animals. Similarly, positive and negative functional connectivity of the WAS-CTX animals with the thalamus was largely reduced or absent, with significant positive connectivity only in the thalamic anterior medial nucleus and limited areas of the midline/intralaminar region, and significant negative functional connectivity noted in limited nuclei of the posterior thalamus (ventral posteromedial nucleus, lateral posterior, posterior). WAS-CTX compared to WAS animals showed a significant negative (rather than positive) functional connectivity of the right pCg/antRS cortex with the anterior amygdala (lateral, basolateral nuclei) and the striatum (dorsal, dorsomedial, lateral). WAS-CTX, unlike WAS

animals, showed no significant functional connectivity of the right pCg/antRS with the parabrachial/Barrington nucleus complex.

However, WAS-CTX compared to WAS animals showed a broader significant positive functional connectivity of the pCg/antRS to the posterior retrosplenial cortex, periaqueductal gray, posterior hippocampus, posterior superior colliculus, deep mesencephalon, and red nucleus.

4. Discussion

Chronic pain states are associated with alterations in multiple, overlapping brain circuits, including compromised descending inhibitory or facilitatory control systems^{29, 76–79} and possible alterations in brainstem neurons projecting to supraspinal centers.⁸⁰ Functional brain mapping has suggested the presence of a cerebral–bladder control network whose neuronal activity differentially responds to bladder filling or voiding^{81, 82}. Regions in this network frequently identified with both functional and structural abnormalities in patients with IC/BPS include sensorimotor regions such as primary somatosensory cortex, supplementary motor cortex, and the thalamus, but also regions deeply engaged in the modulation of emotions such as the cingulate, insula, and amygdala.^{16–18, 20–24, 83, 84}

In our rodent model, WAS animals compared to SHAM demonstrated a decreased pressure threshold and VMR threshold triggering the voiding phase. Our prior study²⁹ demonstrated that WAS compared to SHAM animals demonstrated significant changes in cerebral activation during passive bladder distension. WAS animals showed greater activation in cortical regions of the central micturition circuit, including the posterior cingulate, anterior retrosplenial, somatosensory, posterior insula, orbital, and anterior secondary ('supplementary' [dummy]) motor cortices, as well as in the thalamus, anterior hypothalamus, parabrachial and Barrington nuclei, and striatum. Significant decreases in rCBF in the WAS vs. SHAM comparison were noted in regions associated with emotional regulation such as the amygdala, posterior hypothalamus and dorsal hippocampus. Reanalysis by ANOVA in our 4 groups confirmed the significant effect of 'STRESS' in all these regions. All these areas play important roles in both the micturition and nociceptive circuits (see reviews^{85–87}). Only the parabrachial/Barrington's nuclear complex²⁹, important in the micturition circuit, did not reach significance by ANOVA, though showing a significant increase in rCBF for the WAS vs. SHAM comparison on t-tests.

As suggested by our previous study²⁵, glutamate appears to play a role in mediating the effects of stress in bladder hyperalgesia, as treatment with CTX in our animal model leads to normalization of pressure and VMR thresholds that trigger voiding phase, suggesting improvements in overall bladder hypersensitivity. On functional brain mapping, both WAS and SHAM groups showed a similar distribution of significant effects (Fig. 2, columns 1 – 2). Here drug-treated compared to drug-naïve animals demonstrated significant increases in rCBF in the above-mentioned 'stress-sensitive' regions, except in limbic regions (e.g. amygdala, ventral striatum, and hypothalamus), the parabrachial/Barrington complex and sensory regions (e.g. somatosensory cortex, sensory thalamus, posterior insula) where significant decreases in rCBF were noted (Figs. 2, 3). A significant 'Stress × Ceftriaxone'

interaction was noted in the pCg/antRS, as well as in the somatosensory cortex, insula, amygdala, hippocampus, hypothalamus and emotional thalamus (Table 1), reflecting an accentuated drug effect in WAS compared to SHAM animals in limbic and sensory regions.

CTX, while not acutely altering CBF, is felt to acutely increase brain metabolism and to alter brain functional connectivity through its actions on the astrocytic GLT-1 transporter.⁸⁸ In our study, we did not image animals during an acute CTX challenge, but rather one day following discontinuation of the drug. However, our main effect of 'CTX' was noted in many of the brain regions reported previously by Zimmer et al. as demonstrating changes in glucose metabolism during an acute CTX challenge.⁸⁸ This included frontal cortex, hippocampus, striatum and thalamus, and to a lesser extent the cerebellum. This suggests that CTX may have elicited a persistent functional remodeling in regions of high GLT-1 expression.

A rapidly expanding literature (greater than 70 publications since 2016) has reported functional and structural abnormalities of the posterior medial cortex (comprising pCg and its neighboring structure the precuneus, a part of the superior parietal lobule) in a number of chronic pain conditions, including IC/BPS, fibromyalgia, somatoform disorder, and chronic pain syndrome, either at the level of regional cerebral perfusion and functional connectivity^{19, 89–102} or gray matter volume.^{103–106} Recent resting state functional magnetic resonance imaging (rs-fMRI) data published by the MAPP consortium has confirmed in a large sample of females with UCPPS a functional disruption of this posterior medial cortex¹⁹. Patients compared to controls showed functional disconnection of the pCg/precuneus from the default network (DMN), but increased functional connectivity to several brain regions implicated in pain, sensory, motor, and emotional regulation. In these patients, altered pCg/precuneus connectivity was associated with pain and urologic symptom intensity, depression, and anxiety.

Within the DMN, the pCg represents a central node that connects widely and heterogeneously across the brain. Its function is multifold, with proposed roles in cognition, attention, pain perception, emotional processing, sensory integration, including bladder filling and urinary urgency.¹⁰⁷ Cross-species cytoarchitectural maps, suggest a correspondence between the human precuneus and the rodent retrosplenial cortex¹⁰⁸, a cortical midline structure which lies immediately caudal to the pCg, and which in rats is considered a central functional hub in the DMN¹⁰⁹. In rodents, the retrosplenial cortex is known to contribute to contextual and spatial learning and memory.¹¹⁰ Findings indicate that retrosplenial cortex here may contribute to episodic memory formation by linking essential sensory stimuli during learning.^{111–113} Recent findings highlight the importance of the retrosplenial cortex also in the regulation of pain^{114–116}, as well as in the regulation of visceral functions and arousal¹¹⁷, as well as in the storage of urine¹¹⁸ and urinary urgency.¹¹⁹ In our study, ANOVA revealed a significant main effect of 'Stress', as well as a significant 'Stress × CTX' interaction in the pCg/antRS, suggesting this region to be sensitive to WAS and to show a differential drug response.

In addition, our data in the WAS rodent model demonstrated significant stress-related alterations in functional connectivity of the pCg/antRS (Fig. 4). Significant positive

functional connectivity of the pCg/antRS was more pronounced in WAS compared to SHAM rats to several of the nodes of the micturition circuit and associated sensory regions, many for which there is evidence of structural connectivity.^{120–123} This was true for anterior midline cortex (prelimbic, anterior cingulate), insular cortex, motor cortex (primary, secondary), hippocampus, anterior thalamus (anteromedial, anteroventral, ventrolateral), parabrachial/Barrington nucleus complex, as well as somatosensory cortex. Negative connectivity was present more extensively in WAS than in SHAM groups in regions of the posterior thalamus and periventricular gray/anterior periaqueductal gray. CTX treatment in WAS animals diminished or reversed the functional connectivity for many of the regions noted to be functionally connected to the pCg/antRS in WAS animals. In particular, functional connectivity turned from positive to negative in the midline prefrontal cortex (prelimbic, anterior cingulate), posterior insula, somatosensory cortex (primary, secondary), amygdala, anterior thalamus, and parabrachial/Barrington nucleus complex, with functional connectivity increasing in the periaqueductal gray.

While our animal model reproduces many of the physiologic, behavioral and brain functional characteristics of IC/BPS, it is unlikely that stress acts as the sole etiological factor in IC/BPS. More likely, stress acts as a vulnerability factor in individuals predisposed to the disease for other reasons such as genetic predisposition, infections, etc. ('stress-diathesis' theory¹²⁴). Animal data supports this concept, where chronic WAS induces bladder hypersensitivity in high-anxiety but not in normal rats.¹²⁵ Thus, additional stresses in adulthood may precipitate full-blown clinical syndromes in vulnerable subjects. Our study did not distinguish between the brain and spinal cord as potential target sites of CTX. Future studies will need to examine such differences.

Finally, it is important to remember that in addition to its role as an antibiotic, and well-established effects in reducing excitotoxicity through increases in astrocytic GLT-1 in the brain and spinal cord,¹²⁶ CEF may act on the nervous system through a number of additional mechanisms.¹²⁷ These include, amongst others, the regulation of genes related to beta-amyloid metabolism, the amelioration of oxidative stress through alterations in levels of glutathione, superoxidase dismutase, Bcl2 and caspases 3 and 9, as well as the increase in levels of brain derived neurotrophic factor and erythropoietin. Hence, in our study, any presumed functional remodeling of the neural circuits within the CNS or spinal cord, may have involved more than simple upregulation of astrocytic GLT-1.

In summary, water avoidance stress in rats, elicited subsequent visceral hypersensitivity during bladder filling as demonstrated by a decreased pressure threshold and VMR threshold triggering the voiding phase. Cerebral perfusion mapping revealed stress effects in brain regions previously noted by others to be responsive to passive bladder filling.^{83, 118, 119} Administration of CTX during stress exposure diminished visceral hypersensitivity and attenuated many of the stress-related functional brain changes within the supraspinal micturition circuit and in overlapping nodes of the limbic and nociceptive systems, including the pCg/antRS, somatosensory cortex, and anterior thalamus. A significant differential effect of CTX on functional connectivity of the pCg/antRS cortex of stressed animals compared to controls was noted. This posterior midline cortical region contributes to pain and to micturition circuits, shows stress effects, and has been reported to demonstrated altered

functionality in IC/BPS patients.^{19, 83} Given the actions of CTX on the glutamate transporter, our results suggest the possibility of glutamatergic pharmacologic strategies in modulating stress-related bladder dysfunction.

Acknowledgements

Funding: This work was supported by a MAPP Research Network grant (U01 DK082370) from the National Institutes of Diabetes and Digestive and Kidney Diseases (NIDDK), National Institutes of Health (NIH), and the MadocksBrown Foundation.

Abbreviations

ANOVA	Analysis of variance
CBF	Cerebral blood flow
CMG	Cystometrogram
CTX	Ceftriaxone
DMN	Default mode network
EAAT-2	Excitatory amino acid transporter 2
GLT-1	Glutamate transporter
IC/BPS	Interstitial cystitis/bladder pain syndrome
IVPmax	Maximum intravesical pressure
MAPP	Multidisciplinary Approach to the Study of Chronic Pelvic Pain
pCg/antRS	Posterior cingulate/anterior retrosplenial
PT	Pressure threshold
rCBF	Regional cerebral blood flow
rs-fMRI	Resting state functional magnetic resonance imaging
UCPPS	Urologic chronic pelvic pain syndrome
VMR	Visceromotor response
WAS	Water avoidance stress

BIBLIOGRAPHY

1. Lai HH, Jemielita T, Sutcliffe S, et al. Characterization of Whole Body Pain in Urological Chronic Pelvic Pain Syndrome at Baseline: A MAPP Research Network Study. *J Urol* 2017;198:622–631. [PubMed: 28373134]
2. Rothrock NE, Lutgendorf SK, Kreder KJ, Ratliff TL, Zimmerman B. Daily stress and symptom exacerbation in interstitial cystitis patients. *Urology* 2001;57:122.
3. Sanford MT, Rodriguez LV. The role of environmental stress on lower urinary tract symptoms. *Curr Opin Urol* 2017;27:268–273. [PubMed: 28376513]

4. Chiu CD, Lee MH, Chen WC, Ho HL, Wu HC. Childhood trauma perpetrated by close others, psychiatric dysfunction, and urological symptoms in patients with interstitial cystitis/bladder pain syndrome. *J Psychosom Res* 2017;93:90–95. [PubMed: 28107899]
5. Naliboff BD, Stephens AJ, Afari N, et al. Widespread Psychosocial Difficulties in Men and Women With Urologic Chronic Pelvic Pain Syndromes: Case-control Findings From the Multidisciplinary Approach to the Study of Chronic Pelvic Pain Research Network. *Urology* 2015;85:1319–1327. [PubMed: 26099876]
6. Nickel JC, Tripp DA, Pontari M, et al. Psychosocial phenotyping in women with interstitial cystitis/painful bladder syndrome: a case control study. *J Urol* 2010;183:167–172. [PubMed: 19913812]
7. Talati A, Ponniah K, Strug LJ, Hodge SE, Fyer AJ, Weissman MM. Panic Disorder, Social Anxiety Disorder, and a Possible Medical Syndrome Previously Linked to Chromosome 13. *Biol Psychiatry* 2007.
8. Naliboff BD, Stephens AJ, Lai HH, et al. Clinical and Psychosocial Predictors of Urological Chronic Pelvic Pain Symptom Change in 1 Year: A Prospective Study from the MAPP Research Network. *J Urol* 2017;198:848–857. [PubMed: 28528930]
9. Perez DL, Barsky AJ, Vago DR, Baslet G, Silbersweig DA. A neural circuit framework for somatosensory amplification in somatoform disorders. *J Neuropsychiatry Clin Neurosci* 2015;27:e40–50. [PubMed: 25716493]
10. Latremoliere A, Woolf CJ. Central sensitization: a generator of pain hypersensitivity by central neural plasticity. *J Pain* 2009;10:895–926. [PubMed: 19712899]
11. Yeh LF, Watanabe M, Sulkes-Cuevas J, Johansen JP. Dysregulation of aversive signaling pathways: a novel circuit endophenotype for pain and anxiety disorders. *Curr Opin Neurobiol* 2017;48:37–44. [PubMed: 28965072]
12. Walitt B, Ceko M, Gracely JL, Gracely RH. Neuroimaging of Central Sensitivity Syndromes: Key Insights from the Scientific Literature. *Curr Rheumatol Rev* 2016;12:55–87. [PubMed: 26717948]
13. Farmer AD, Aziz Q, Tack J, Van Oudenhove L. The future of neuroscientific research in functional gastrointestinal disorders: integration towards multidimensional (visceral) pain endophenotypes? *J Psychosom Res* 2010;68:475–481. [PubMed: 20403507]
14. Kilpatrick LA, Ornitz E, Ibrahimovic H, et al. Gating of sensory information differs in patients with interstitial cystitis/painful bladder syndrome. *J Urol* 2010;184:958–963. [PubMed: 20643444]
15. Twiss C, Kilpatrick L, Craske M, et al. Increased startle responses in interstitial cystitis: evidence for central hyperresponsiveness to visceral related threat. *J Urol* 2009;181:2127–2133. [PubMed: 19286199]
16. Woodworth D, Mayer E, Leu K, et al. Unique Microstructural Changes in the Brain Associated with Urological Chronic Pelvic Pain Syndrome (UCPPS) Revealed by Diffusion Tensor MRI, Super-Resolution Track Density Imaging, and Statistical Parameter Mapping: A MAPP Network Neuroimaging Study. *PLoS ONE* 2015;10:e0140250. [PubMed: 26460744]
17. Kutch JJ, Yani MS, Asavasopon S, et al. Altered resting state neuromotor connectivity in men with chronic prostatitis/chronic pelvic pain syndrome: A MAPP: Research Network Neuroimaging Study. *Neuroimage Clin* 2015;8:493–502. [PubMed: 26106574]
18. Huang L, Kutch JJ, Ellingson BM, et al. Brain white matter changes associated with urological chronic pelvic pain syndrome: multisite neuroimaging from a MAPP case-control study. *Pain* 2016;157:2782–2791. [PubMed: 27842046]
19. Martucci KT, Shirer WR, Bagarinao E, et al. The posterior medial cortex in urologic chronic pelvic pain syndrome: detachment from default mode network—a resting-state study from the MAPP Research Network. *Pain* 2015;156:1755–1764. [PubMed: 26010458]
20. Farmer MA, Huang L, Martucci K, et al. Brain White Matter Abnormalities in Female Interstitial Cystitis/Bladder Pain Syndrome: A MAPP Network Neuroimaging Study. *J Urol* 2015;194:118–126. [PubMed: 25711200]
21. Bagarinao E, Johnson KA, Martucci KT, et al. Preliminary structural MRI based brain classification of chronic pelvic pain: A MAPP network study. *Pain* 2014;155:2502–2509. [PubMed: 25242566]
22. Kleinhans NM, Yang CC, Strachan ED, Buchwald DS, Maravilla KR. Alterations in Connectivity on Functional Magnetic Resonance Imaging with Provocation of Lower Urinary Tract Symptoms:

- A MAPP Research Network Feasibility Study of Urological Chronic Pelvic Pain Syndromes. *J Urol* 2016;195:639–645. [PubMed: 26497778]
23. Kairys AE, Schmidt-Wilcke T, Puiu T, et al. Increased brain gray matter in the primary somatosensory cortex is associated with increased pain and mood disturbance in patients with interstitial cystitis/painful bladder syndrome. *J Urol* 2015;193:131–137. [PubMed: 25132239]
 24. Kilpatrick LA, Kutch JJ, Tillisch K, et al. Alterations in resting state oscillations and connectivity in sensory and motor networks in women with interstitial cystitis/painful bladder syndrome. *J Urol* 2014;192:947–955. [PubMed: 24681331]
 25. Ackerman AL, Jellison FC, Lee UJ, Bradesi S, Rodriguez LV. The Glt1 glutamate receptor mediates the establishment and perpetuation of chronic visceral pain in an animal model of stress-induced bladder hyperalgesia. *Am J Physiol Renal Physiol* 2016;310:F628–F636. [PubMed: 26697981]
 26. Gao Y, Zhang R, Chang HH, Rodriguez LV. The role of C-fibers in the development of chronic psychological stress induced enhanced bladder sensations and nociceptive responses: A multidisciplinary approach to the study of urologic chronic pelvic pain syndrome (MAPP) research network study. *NeuroUrol Urodyn* 2017.
 27. Lee UJ, Ackerman AL, Wu A, et al. Chronic psychological stress in high-anxiety rats induces sustained bladder hyperalgesia. *Physiol Behav* 2015;139:541–548. [PubMed: 25449389]
 28. Matos R, Serrao P, Rodriguez L, Birder LA, Cruz F, Charrua A. The water avoidance stress induces bladder pain due to a prolonged alpha1A adrenoceptor stimulation. *Naunyn Schmiedebergs Arch Pharmacol* 2017;390:839–844. [PubMed: 28569366]
 29. Wang Z, Chang HH, Gao Y, et al. Effects of water avoidance stress on peripheral and central responses during bladder filling in the rat: A multidisciplinary approach to the study of urologic chronic pelvic pain syndrome (MAPP) research network study. *PLoS ONE* 2017;12:e0182976. [PubMed: 28886046]
 30. Koziol JA. Epidemiology of interstitial cystitis. *Urol Clin North Am* 1994;21:7–20. [PubMed: 8284848]
 31. Lutgendorf SK, Kreder KJ, Rothrock NE, Ratliff TL, Zimmerman B. Stress and symptomatology in patients with interstitial cystitis: a laboratory stress model. *J Urol* 2000;164:1265–1269. [PubMed: 10992377]
 32. Nickel JC, Shoskes D, Irvine-Bird K. Clinical phenotyping of women with interstitial cystitis/painful bladder syndrome: a key to classification and potentially improved management. *J Urol* 2009;182:155–160. [PubMed: 19447429]
 33. Nickel JC, Tripp DA, Pontari M, et al. Interstitial cystitis/painful bladder syndrome and associated medical conditions with an emphasis on irritable bowel syndrome, fibromyalgia and chronic fatigue syndrome. *J Urol* 2010;184:1358–1363. [PubMed: 20719340]
 34. Rothrock NE, Lutgendorf SK, Kreder KJ, Ratliff T, Zimmerman B. Stress and symptoms in patients with interstitial cystitis: a life stress model. *Urology* 2001;57:422–427. [PubMed: 11248609]
 35. Sanses T, McCabe P, Zhong L, et al. Sensory mapping of pelvic dermatomes in women with interstitial cystitis/bladder pain syndrome. *NeuroUrol Urodyn* 2017.
 36. Sanses TV, Chelimsky G, McCabe NP, et al. The Pelvis and Beyond: Musculoskeletal Tender Points in Women With Chronic Pelvic Pain. *Clin J Pain* 2016;32:659–665. [PubMed: 26491938]
 37. Lai HH, Gardner V, Ness TJ, Gereau RWt. Segmental hyperalgesia to mechanical stimulus in interstitial cystitis/bladder pain syndrome: evidence of central sensitization. *J Urol* 2014;191:1294–1299. [PubMed: 24316091]
 38. Lowenstein L, Kenton K, Mueller ER, et al. Patients with painful bladder syndrome have altered response to thermal stimuli and catastrophic reaction to painful experiences. *NeuroUrol Urodyn* 2009;28:400–404. [PubMed: 19191279]
 39. Ness TJ, Powell-Boone T, Cannon R, Lloyd LK, Fillingim RB. Psychophysical evidence of hypersensitivity in subjects with interstitial cystitis. *J Urol* 2005;173:1983–1987. [PubMed: 15879797]
 40. Popoli M, Yan Z, McEwen BS, Sanacora G. The stressed synapse: the impact of stress and glucocorticoids on glutamate transmission. *Nat Rev Neurosci* 2012;13:22–37.

41. Stephens RL Jr. Glutamate transporter activators as anti-nociceptive agents. *Eurasian J Med* 2011;43:182–185. [PubMed: 25610189]
42. Sung B, Lim G, Mao J. Altered expression and uptake activity of spinal glutamate transporters after nerve injury contribute to the pathogenesis of neuropathic pain in rats. *J Neurosci* 2003;23:2899–2910. [PubMed: 12684477]
43. Crock LW, Stemler KM, Song DG, et al. Metabotropic glutamate receptor 5 (mGluR5) regulates bladder nociception. *Mol Pain* 2012;8:20. [PubMed: 22449017]
44. As-Sanie S, Kim J, Schmidt-Wilcke T, et al. Functional Connectivity is Associated With Altered Brain Chemistry in Women With Endometriosis-Associated Chronic Pelvic Pain. *J Pain* 2016;17:1–13. [PubMed: 26456676]
45. Harris RE, Napadow V, Huggins JP, et al. Pregabalin rectifies aberrant brain chemistry, connectivity, and functional response in chronic pain patients. *Anesthesiology* 2013;119:1453–1464. [PubMed: 24343290]
46. Harris RE, Sundgren PC, Craig AD, et al. Elevated insular glutamate in fibromyalgia is associated with experimental pain. *Arthritis Rheum* 2009;60:3146–3152. [PubMed: 19790053]
47. Petrou M, Pop-Busui R, Foerster BR, et al. Altered excitation-inhibition balance in the brain of patients with diabetic neuropathy. *Acad Radiol* 2012;19:607–612. [PubMed: 22463961]
48. Valdes M, Collado A, Bargallo N, et al. Increased glutamate/glutamine compounds in the brains of patients with fibromyalgia: a magnetic resonance spectroscopy study. *Arthritis Rheum* 2010;62:1829–1836. [PubMed: 20191578]
49. Pyke T, Osmotherly PG, Baines S. Measuring Glutamate Levels in the Brains of Fibromyalgia Patients and a Potential Role for Glutamate in the Pathophysiology of Fibromyalgia Symptoms: A Systematic Review. *Clin J Pain* 2016.
50. Altar CA, Vawter MP, Ginsberg SD. Target identification for CNS diseases by transcriptional profiling. *Neuropsychopharmacology* 2009;34:18–54. [PubMed: 18923405]
51. Lee Y, Gaskins D, Anand A, Shekhar A. Glia mechanisms in mood regulation: a novel model of mood disorders. *Psychopharmacology (Berl)* 2007;191:55–65. [PubMed: 17225169]
52. McEwen BS, Eiland L, Hunter RG, Miller MM. Stress and anxiety: structural plasticity and epigenetic regulation as a consequence of stress. *Neuropharmacology* 2012;62:3–12. [PubMed: 21807003]
53. Yang CH, Huang CC, Hsu KS. Behavioral stress enhances hippocampal CA1 long-term depression through the blockade of the glutamate uptake. *J Neurosci* 2005;25:4288–4293. [PubMed: 15858055]
54. Zink M, Vollmayr B, Gebicke-Haerter PJ, Henn FA. Reduced expression of glutamate transporters vGluT1, EAAT2 and EAAT4 in learned helpless rats, an animal model of depression. *Neuropharmacology* 2010;58:465–473. [PubMed: 19747495]
55. Yang M, Roman K, Chen DF, Wang ZG, Lin Y, Stephens RL, Jr. GLT-1 overexpression attenuates bladder nociception and local/cross-organ sensitization of bladder nociception. *Am J Physiol Renal Physiol* 2011;300:F1353–1359. [PubMed: 21429971]
56. Lin Y, Roman K, Foust KD, Kaspar BK, Bailey MT, Stephens RL. Glutamate Transporter GLT-1 Upregulation Attenuates Visceral Nociception and Hyperalgesia via Spinal Mechanisms Not Related to Anti-Inflammatory or Probiotic Effects. *Pain Res Treat* 2011;2011:507029. [PubMed: 22220274]
57. Mishra SP, Shukla SK, Pandey BL. A preliminary evaluation of comparative effectiveness of riluzole in therapeutic regimen for irritable bowel syndrome. *Asian Pac J Trop Biomed* 2014;4:S335–340. [PubMed: 25183107]
58. Smith AL, Leung J, Kun S, et al. The effects of acute and chronic psychological stress on bladder function in a rodent model. *Urology* 2011;78:967 e961–967.
59. Stewart WF, Van Rooyen JB, Cundiff GW, et al. Prevalence and burden of overactive bladder in the United States. *World J Urol* 2003;20:327–336. [PubMed: 12811491]
60. National-Research-Council-(US)-Committee-for-the-Update-of-the-Guide-for-the-Care-and-Use-of-Laboratory-Animals Guide for the Care and Use of Laboratory Animals, 8th ed. Washington, DC: National Academies Press, 2011.

61. Bradesi S, Schwetz I, Ennes HS, et al. Repeated exposure to water avoidance stress in rats: a new model for sustained visceral hyperalgesia. *Am J Physiol Gastrointest Liver Physiol* 2005;289:G42–53. [PubMed: 15746211]
62. Wang Z, Ocampo MA, Pang RD, et al. Alterations in prefrontal-limbic functional activation and connectivity in chronic stress-induced visceral hyperalgesia. *PLoS ONE* 2013;8:e59138. [PubMed: 23527114]
63. Baek K, Shim WH, Jeong J, et al. Layer-specific interhemispheric functional connectivity in the somatosensory cortex of rats: resting state electrophysiology and fMRI studies. *Brain Struct Funct* 2016;221:2801–2815. [PubMed: 26077581]
64. Kalthoff D, Po C, Wiedermann D, Hoehn M. Reliability and spatial specificity of rat brain sensorimotor functional connectivity networks are superior under sedation compared with general anesthesia. *NMR Biomed* 2013;26:638–650. [PubMed: 23303725]
65. Magnuson ME, Thompson GJ, Pan WJ, Keilholz SD. Time-dependent effects of isoflurane and dexmedetomidine on functional connectivity, spectral characteristics, and spatial distribution of spontaneous BOLD fluctuations. *NMR Biomed* 2014;27:291–303. [PubMed: 24449532]
66. Martin C, Martindale J, Berwick J, Mayhew J. Investigating neural-hemodynamic coupling and the hemodynamic response function in the awake rat. *Neuroimage* 2006;32:33–48. [PubMed: 16725349]
67. Holschneider DP, Maarek JM, Harimoto J, Yang J, Scremin OU. An implantable bolus infusion pump for use in freely moving, nontethered rats. *Am J Physiol Heart Circ Physiol* 2002;283:H1713–1719. [PubMed: 12234827]
68. Goldman H, Sapirstein LA. Brain blood flow in the conscious and anesthetized rat. *Am J Physiol* 1973;224:122–126. [PubMed: 4566847]
69. Patlak CS, Blasberg RG, Fenstermacher JD. An evaluation of errors in the determination of blood flow by the indicator fractionation and tissue equilibration (Kety) methods. *J Cereb Blood Flow Metab* 1984;4:47–60. [PubMed: 6363433]
70. Sakurada O, Kennedy C, Jehle J, Brown JD, Carbin GL, Sokoloff L. Measurement of local cerebral blood flow with iodo [14C] antipyrine. *Am J Physiol* 1978;234:H59–66. [PubMed: 623275]
71. Stumpf WE, Solomon HF. *Autoradiography and Correlative Imaging*. New York: Academic Press, 1995.
72. Friston K. *Neurology atMgatWDoC. Statistical Parametric Mapping (SPM99)*; <http://www.fil.ion.ucl.ac.uk/spm/> 1999.
73. Nguyen PT, Holschneider DP, Maarek JM, Yang J, Mandelkern MA. Statistical parametric mapping applied to an autoradiographic study of cerebral activation during treadmill walking in rats. *Neuroimage* 2004;23:252–259. [PubMed: 15325372]
74. Paxinos G, Watson C. *The Rat Brain in Stereotactic Coordinates*, 6th ed. New York: Elsevier Academic Press, 2007.
75. Wang Z, Pang RD, Hernandez M, Ocampo MA, Holschneider DP. Anxiolytic-like effect of pregabalin on unconditioned fear in the rat: an autoradiographic brain perfusion mapping and functional connectivity study. *Neuroimage* 2012;59:4168–4188. [PubMed: 22155030]
76. de Leeuw R, Albuquerque R, Okeson J, Carlson C. The contribution of neuroimaging techniques to the understanding of supraspinal pain circuits: implications for orofacial pain. *Oral Surg Oral Med Oral Pathol Oral Radiol Endod* 2005;100:308–314. [PubMed: 16122658]
77. Porreca F, Ossipov MH, Gebhart GF. Chronic pain and medullary descending facilitation. *Trends Neurosci* 2002;25:319–325. [PubMed: 12086751]
78. Coghill RC, Sang CN, Maisog JM, Iadarola MJ. Pain intensity processing within the human brain: a bilateral, distributed mechanism. *J Neurophysiol* 1999;82:1934–1943. [PubMed: 10515983]
79. Mennini T, Testa R. Are descending control pathways of the lower urinary tract and pain overlapping systems? *Cent Nerv Syst Agents Med Chem* 2010;10:113–147. [PubMed: 20518728]
80. Jensen TS. Opioids in the brain: supraspinal mechanisms in pain control. *Acta Anaesthesiol Scand* 1997;41:123–132. [PubMed: 9061095]
81. Griffiths DJ, Fowler CJ. The micturition switch and its forebrain influences. *Acta Physiol (Oxf)* 2013;207:93–109. [PubMed: 23164237]

82. Krhut J, Holy P, Tintera J, Zachoval R, Zvara P. Brain activity during bladder filling and pelvic floor muscle contractions: a study using functional magnetic resonance imaging and synchronous urodynamics. *Int J Urol* 2014;21:169–174. [PubMed: 23815526]
83. Deutsch G, Deshpande H, Frolich MA, Lai HH, Ness TJ. Bladder Distension Increases Blood Flow in Pain Related Brain Structures in Subjects with Interstitial Cystitis. *J Urol* 2016;196:902–910. [PubMed: 27018508]
84. Delgado PL. Common pathways of depression and pain. *J Clin Psychiatry* 2004;65 Suppl 12:16–19.
85. Griffiths D. Neural control of micturition in humans: a working model. *Nat Rev Urol* 2015;12:695–705. [PubMed: 26620610]
86. de Groat WC, Griffiths D, Yoshimura N. Neural control of the lower urinary tract. *Compr Physiol* 2015;5:327–396. [PubMed: 25589273]
87. Peirs C, Seal RP. Neural circuits for pain: Recent advances and current views. *Science* 2016;354:578–584. [PubMed: 27811268]
88. Zimmer ER, Parent MJ, Souza DG, et al. [(18)F]FDG PET signal is driven by astroglial glutamate transport. *Nat Neurosci* 2017;20:393–395. [PubMed: 28135241]
89. Zhang S, Wu W, Huang G, et al. Resting-state connectivity in the default mode network and insula during experimental low back pain. *Neural Regen Res* 2014;9:135–142. [PubMed: 25206794]
90. Vanneste S, Ost J, Van Havenbergh T, De Ridder D. Resting state electrical brain activity and connectivity in fibromyalgia. *PLoS ONE* 2017;12:e0178516. [PubMed: 28650974]
91. Nielsen FA, Balslev D, Hansen LK. Mining the posterior cingulate: segregation between memory and pain components. *Neuroimage* 2005;27:520–532. [PubMed: 15946864]
92. Lopez-Sola M, Woo CW, Pujol J, et al. Towards a neurophysiological signature for fibromyalgia. *Pain* 2017;158:34–47. [PubMed: 27583567]
93. Hemington KS, Wu Q, Kucyi A, Inman RD, Davis KD. Abnormal cross-network functional connectivity in chronic pain and its association with clinical symptoms. *Brain Struct Funct* 2016;221:4203–4219. [PubMed: 26669874]
94. Freund W, Wunderlich AP, Stuber G, et al. Different activation of opercular and posterior cingulate cortex (PCC) in patients with complex regional pain syndrome (CRPS I) compared with healthy controls during perception of electrically induced pain: a functional MRI study. *Clin J Pain* 2010;26:339–347. [PubMed: 20393270]
95. Flodin P, Martinsen S, Lofgren M, Bileviciute-Ljungar I, Kosek E, Fransson P. Fibromyalgia is associated with decreased connectivity between pain- and sensorimotor brain areas. *Brain Connect* 2014;4:587–594. [PubMed: 24998297]
96. Boeckle M, Schrimpf M, Liegl G, Pieh C. Neural correlates of somatoform disorders from a meta-analytic perspective on neuroimaging studies. *Neuroimage Clin* 2016;11:606–613. [PubMed: 27182487]
97. Becker C, Vogt K, Ibinson J. Posterior cingulate connectivity changes during acute and chronic pain. *The Journal of Pain* 2017;18:S56.
98. Wik G, Fischer H, Finer B, Bragee B, Kristianson M, Fredrikson M. Retrosplenial cortical deactivation during painful stimulation of fibromyalgic patients. *Int J Neurosci* 2006;116:1–8. [PubMed: 16318995]
99. Hall GB, Kamath MV, Collins S, et al. Heightened central affective response to visceral sensations of pain and discomfort in IBS. *Neurogastroenterol Motil* 2010;22:276–e280. [PubMed: 20003075]
100. Hong JY, Naliboff B, Labus JS, et al. Altered brain responses in subjects with irritable bowel syndrome during cued and uncued pain expectation. *Neurogastroenterol Motil* 2016;28:127–138. [PubMed: 26526698]
101. Tadic SD, Griffiths D, Schaefer W, Cheng CI, Resnick NM. Brain activity measured by functional magnetic resonance imaging is related to patient reported urgency urinary incontinence severity. *J Urol* 2010;183:221–228. [PubMed: 19913803]
102. Gonzalez-Roldan AM, Bomba IC, Diesch E, Montoya P, Flor H, Kamping S. Controllability and hippocampal activation during pain expectation in fibromyalgia syndrome. *Biol Psychol* 2016;121:39–48. [PubMed: 27678310]

103. Emerson NM, Zeidan F, Lobanov OV, et al. Pain sensitivity is inversely related to regional grey matter density in the brain. *Pain* 2014;155:566–573. [PubMed: 24333778]
104. Hubbard CS, Becerra L, Heinz N, et al. Abdominal Pain, the Adolescent and Altered Brain Structure and Function. *PLoS ONE* 2016;11:e0156545. [PubMed: 27244227]
105. Lin C, Lee SH, Weng HH. Gray Matter Atrophy within the Default Mode Network of Fibromyalgia: A Meta-Analysis of Voxel-Based Morphometry Studies. *Biomed Res Int* 2016;2016:7296125. [PubMed: 28105430]
106. Fallon N, Alghamdi J, Chiu Y, Sluming V, Nurmikko T, Stancak A. Structural alterations in brainstem of fibromyalgia syndrome patients correlate with sensitivity to mechanical pressure. *Neuroimage Clin* 2013;3:163–170. [PubMed: 24179860]
107. Buckner RL, Andrews-Hanna JR, Schacter DL. The brain's default network: anatomy, function, and relevance to disease. *Ann N Y Acad Sci* 2008;1124:1–38. [PubMed: 18400922]
108. Vogt BA, Paxinos G. Cytoarchitecture of mouse and rat cingulate cortex with human homologies. *Brain Struct Funct* 2014;219:185–192. [PubMed: 23229151]
109. Ash JA, Lu H, Taxier LR, et al. Functional connectivity with the retrosplenial cortex predicts cognitive aging in rats. *Proc Natl Acad Sci U S A* 2016;113:12286–12291. [PubMed: 27791017]
110. Vann SD, Aggleton JP, Maguire EA. What does the retrosplenial cortex do? *Nat Rev Neurosci* 2009;10:792–802. [PubMed: 19812579]
111. Robinson S, Todd TP, Pasternak AR, et al. Chemogenetic silencing of neurons in retrosplenial cortex disrupts sensory preconditioning. *J Neurosci* 2014;34:10982–10988. [PubMed: 25122898]
112. Robinson S, Keene CS, Iaccarino HF, Duan D, Bucci DJ. Involvement of retrosplenial cortex in forming associations between multiple sensory stimuli. *Behav Neurosci* 2011;125:578–587. [PubMed: 21688884]
113. Todd TP, Huszar R, DeAngeli NE, Bucci DJ. Higher-order conditioning and the retrosplenial cortex. *Neurobiol Learn Mem* 2016;133:257–264. [PubMed: 27208598]
114. Brito RG, Santos PL, Prado DS, et al. Citronellol reduces orofacial nociceptive behaviour in mice - evidence of involvement of retrosplenial cortex and periaqueductal grey areas. *Basic Clin Pharmacol Toxicol* 2013;112:215–221. [PubMed: 23035741]
115. Goffaux P, Girard-Tremblay L, Marchand S, Daigle K, Whittingstall K. Individual differences in pain sensitivity vary as a function of precuneus reactivity. *Brain Topogr* 2014;27:366–374. [PubMed: 23636269]
116. Reis GM, Fais RS, Prado WA. The antinociceptive effect of stimulating the retrosplenial cortex in the rat tail-flick test but not in the formalin test involves the rostral anterior cingulate cortex. *Pharmacol Biochem Behav* 2015;131:112–118. [PubMed: 25687372]
117. Wang J, Nie B, Duan S, Zhu H, Liu H, Shan B. Functionally Brain Network Connected to the Retrosplenial Cortex of Rats Revealed by 7T fMRI. *PLoS ONE* 2016;11:e0146535. [PubMed: 26745803]
118. Tai C, Wang J, Jin T, et al. Brain switch for reflex micturition control detected by FMRI in rats. *J Neurophysiol* 2009;102:2719–2730. [PubMed: 19741099]
119. Kuitz-Buschbeck JP, Gilster R, van der Horst C, Hamann M, Wolff S, Jansen O. Control of bladder sensations: an fMRI study of brain activity and effective connectivity. *Neuroimage* 2009;47:18–27. [PubMed: 19371782]
120. van Groen T, Wyss JM. Connections of the retrosplenial dysgranular cortex in the rat. *J Comp Neurol* 1992;315:200–216. [PubMed: 1545009]
121. Van Groen T, Wyss JM. Connections of the retrosplenial granular b cortex in the rat. *J Comp Neurol* 2003;463:249–263. [PubMed: 12820159]
122. Olson CR, Musil SY. Topographic organization of cortical and subcortical projections to posterior cingulate cortex in the cat: evidence for somatic, ocular, and complex subregions. *J Comp Neurol* 1992;324:237–260. [PubMed: 1430331]
123. Shibata H Organization of projections of rat retrosplenial cortex to the anterior thalamic nuclei. *Eur J Neurosci* 1998;10:3210–3219. [PubMed: 9786214]
124. Monroe SM, Simons AD. Diathesis-stress theories in the context of life stress research: implications for the depressive disorders. *Psychol Bull* 1991;110:406–425. [PubMed: 1758917]

125. Robbins MT, DeBerry J, Ness TJ. Chronic psychological stress enhances nociceptive processing in the urinary bladder in high-anxiety rats. *Physiol Behav* 2007;91:544–550. [PubMed: 17521683]
126. Rothstein JD, Patel S, Regan MR, et al. Beta-lactam antibiotics offer neuroprotection by increasing glutamate transporter expression. *Nature* 2005;433:73–77. [PubMed: 15635412]
127. Tai CH, Bellesi M, Chen AC, et al. A new avenue for treating neuronal diseases: Ceftriaxone, an old antibiotic demonstrating behavioral neuronal effects. *Behav Brain Res* 2019;364:149–156. [PubMed: 30768995]
128. Griffiths D Functional imaging of structures involved in neural control of the lower urinary tract. *Handb Clin Neurol* 2015;130:121–133. [PubMed: 26003241]
129. de Groat WC, Yoshimura N. Anatomy and physiology of the lower urinary tract. *Handb Clin Neurol* 2015;130:61–108. [PubMed: 26003239]

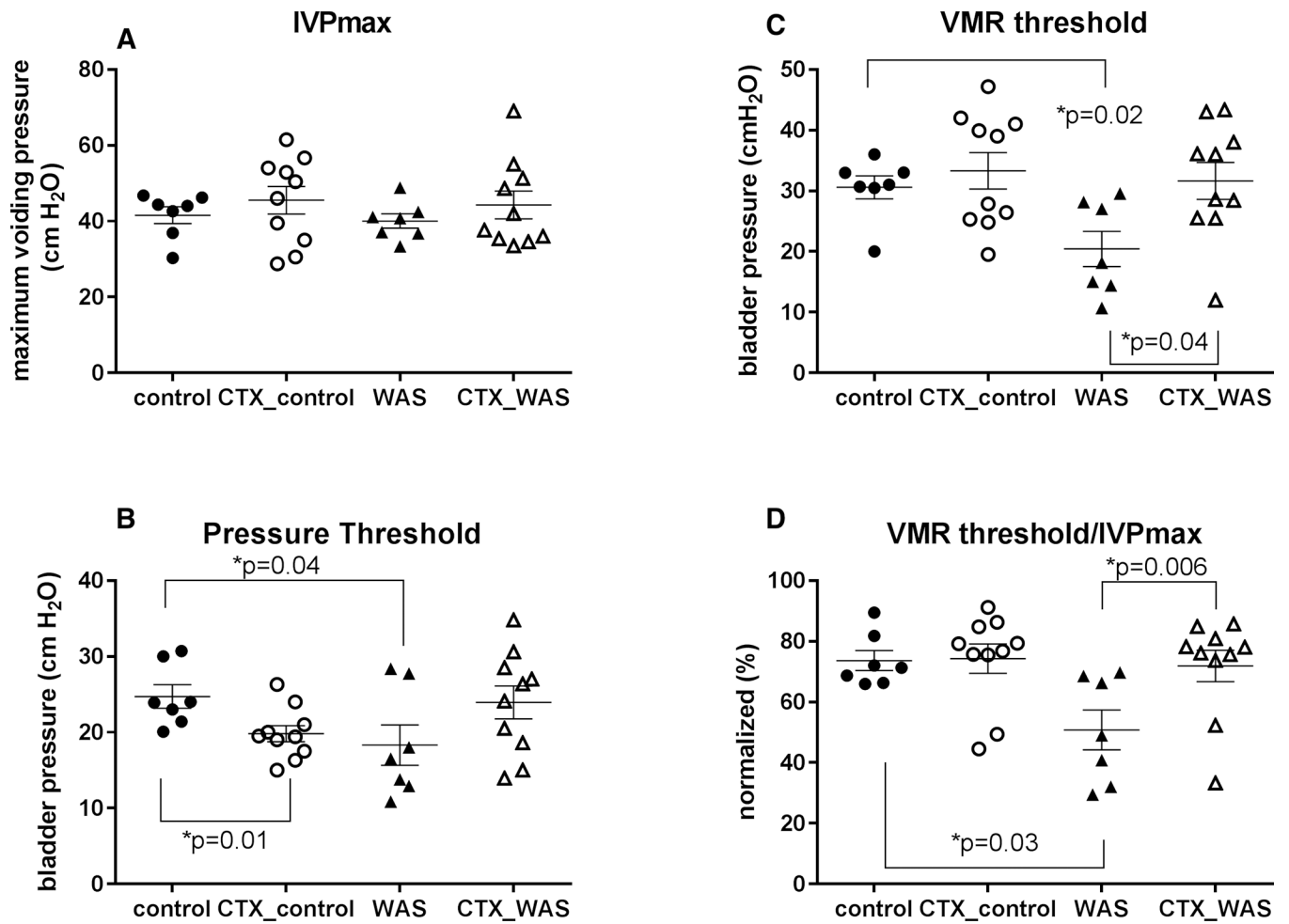


Figure 1: Statistical analysis of the effects of CTX on cystometrogram and visceromotor reflex (average \pm standard error) recordings during bladder infusion.

Shown are the tracings of (A) maximum intravesical voiding pressure (IVPmax), (B) pressure threshold to first void/leak, (C) VMR threshold, and (D) VMR threshold/IVPmax for WAS and SHAM (control) animals in the presence or absence of CTX.

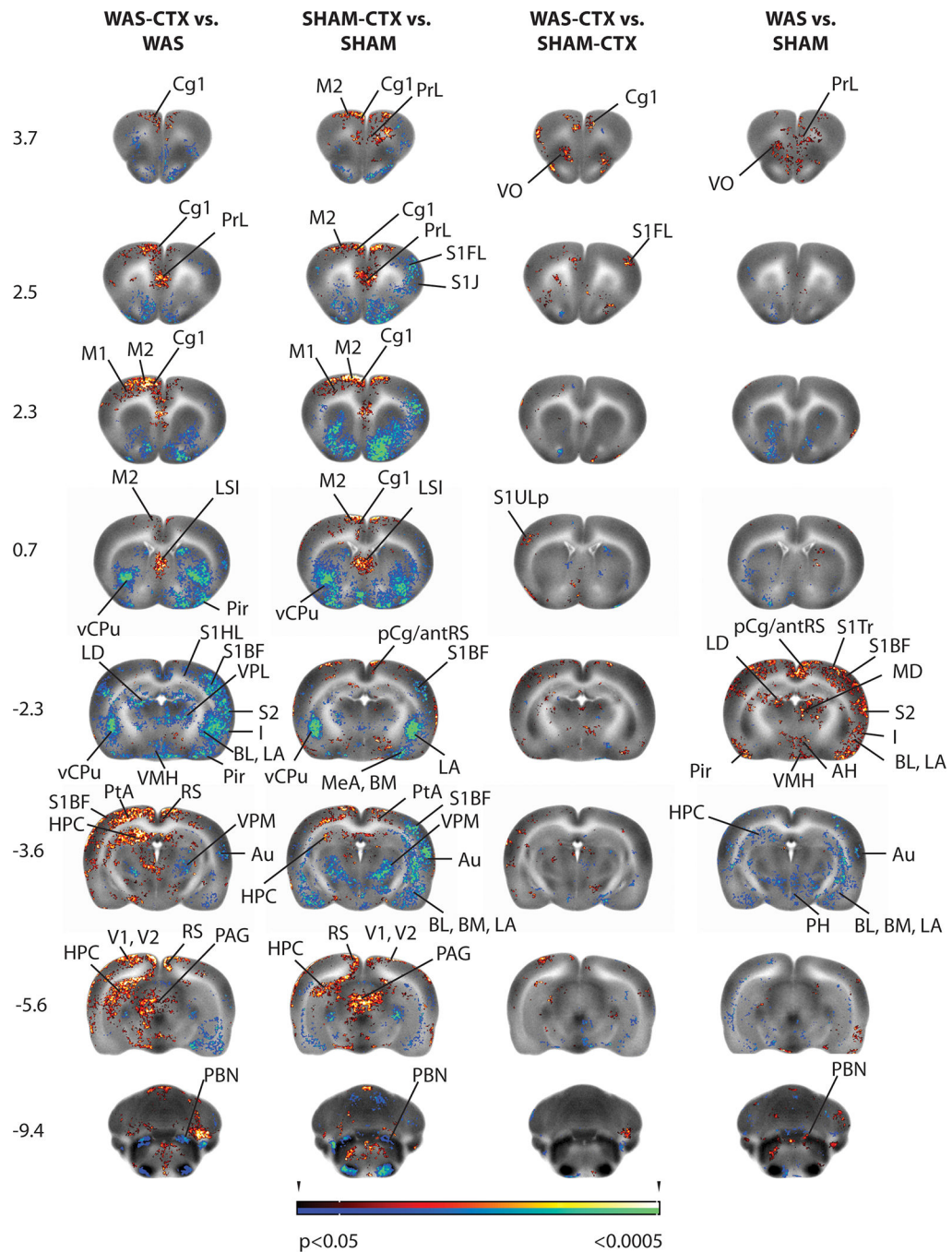


Figure 2: Brain regions showing significant between-group differences in t-tests. Shown are statistical parametric maps showing significant difference in brain activation in sedated WAS rats compared to controls during bladder filling with and without prior exposure to ceftriaxone (CTX). Changes in regional cerebral blood flow related tissue radioactivity are depicted on representative coronal sections (anterior–posterior coordinates relative to the bregma) of the template brain. Color-coded overlays show statistically significant group differences, with red and blue colors showing positive and negative

changes, respectively ($P < 0.05$ at the voxel level for clusters of > 100 contiguous voxels).

Abbreviations are based on the rat brain atlas⁷⁴ with modifications.

Acb n. acumbens AH anterior hypothalamus Au auditory cx BL basolateral amygdala BLA basolateral amygdala BM basomedial amygdala Cg1 dorsal anterior cingulate cx pCg/antRS post. cingulate/ ant. retrosplenial cx CPu striatum dmCPu dorsomedial striatum HPC hippocampus I insula LA lateral amygdala LCC locus coeruleus complex LD lateral dorsal thalamic n. LO lateral orbital cx LSI lateral septum M1 primary motor cx M2 secondary motor cx MD mediodorsal thalamic n. MeA medial amygdala MG medial geniculate pCg posterior cingulate cx PAG periaqueductal gray, PBN parabrachial n. PMCo cortical amygdala Pir piriform cortex PrL prelimbic cx PtA parietal association cx RS retrosplenial cx S1BF primary somatosens. cx barrel field area S1FL primary somatosens. cx forelimb area S1J primary somatosens. cx jaw area S1Tr primary somatosens. cx trunk area S1ULp primary somatosens. cx upper lip area S2 secondary somatosens. cx Sim simple cerebellar lobule SO superior olive STN subthalamic n. V1 primary visual cx V2 secondary visual cx vCPu ventral striatum VL ventrolateral thalamic n. VMH ventromedial hypothalamus VO ventral orbital cx VPL ventral post. lateral thalamic n. VPL/VPM ventral post. lateral/ventral post. medial thalamic n. VPM ventral posterior medial thalamic n. ZI zona incerta

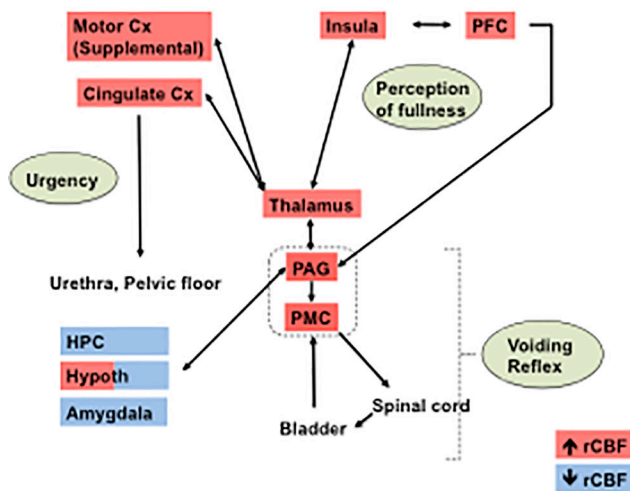
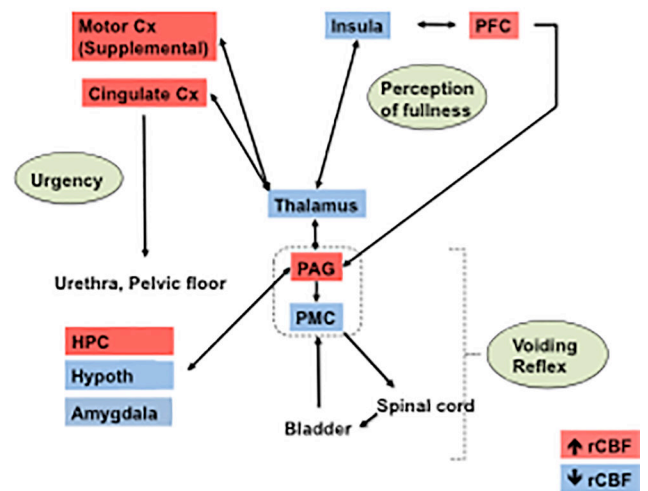
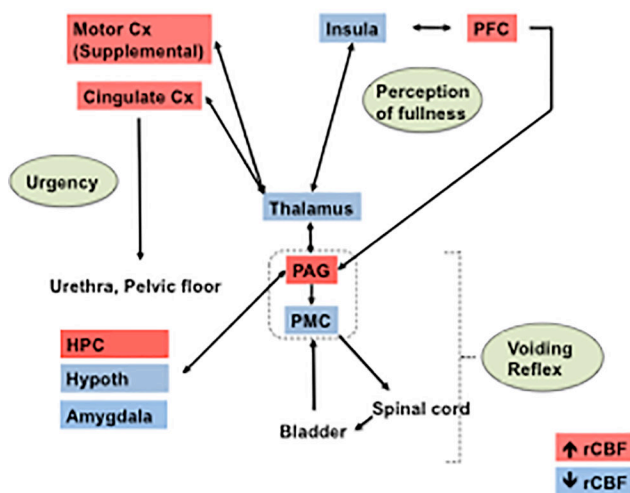
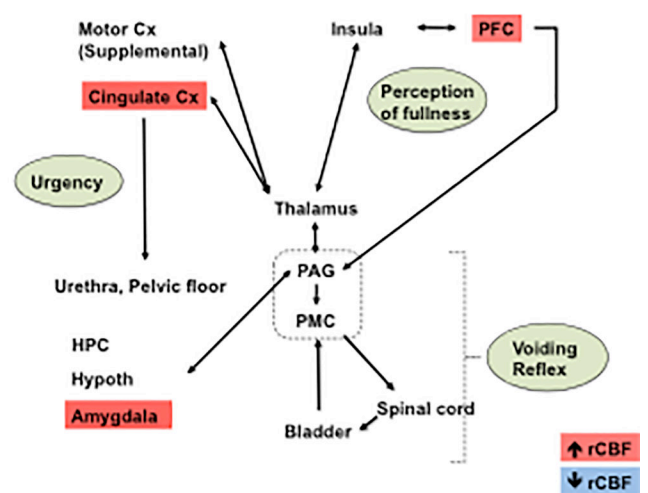
WAS vs. SHAM**WAS-CTX vs. WAS****SHAM-CTX vs. SHAM****WAS-CTX vs. SHAM-CTX**

Figure 3: Summary of the significant changes in regional cerebral blood flow (rCBF) of (A) WAS versus SHAM rats, (B) WAS-CTX versus WAS rats, (C) SHAM-CTX versus SHAM, (D) WAS-CTX versus SHAM-CTX, and during passive bladder filling as related to a simplified model of the micturition circuit. Data are summarized from the SPM analysis shown in Fig. 2, with red indicating significant increases in rCBF and blue indicating significant decreases in rCBF. Abbreviations: CTX (ceftriaxone), Cx (cortex), HPC (hippocampus), PFC (prefrontal cortex), PAG (periaqueductal gray), PMC (pontine micturition center, parabrachial/Barrington nucleus complex). Note: Cingulate cortex refers to the anterior/mid cingulate. Adapted from Griffiths¹²⁸ and DeGroat and Yoshimura.¹²⁹

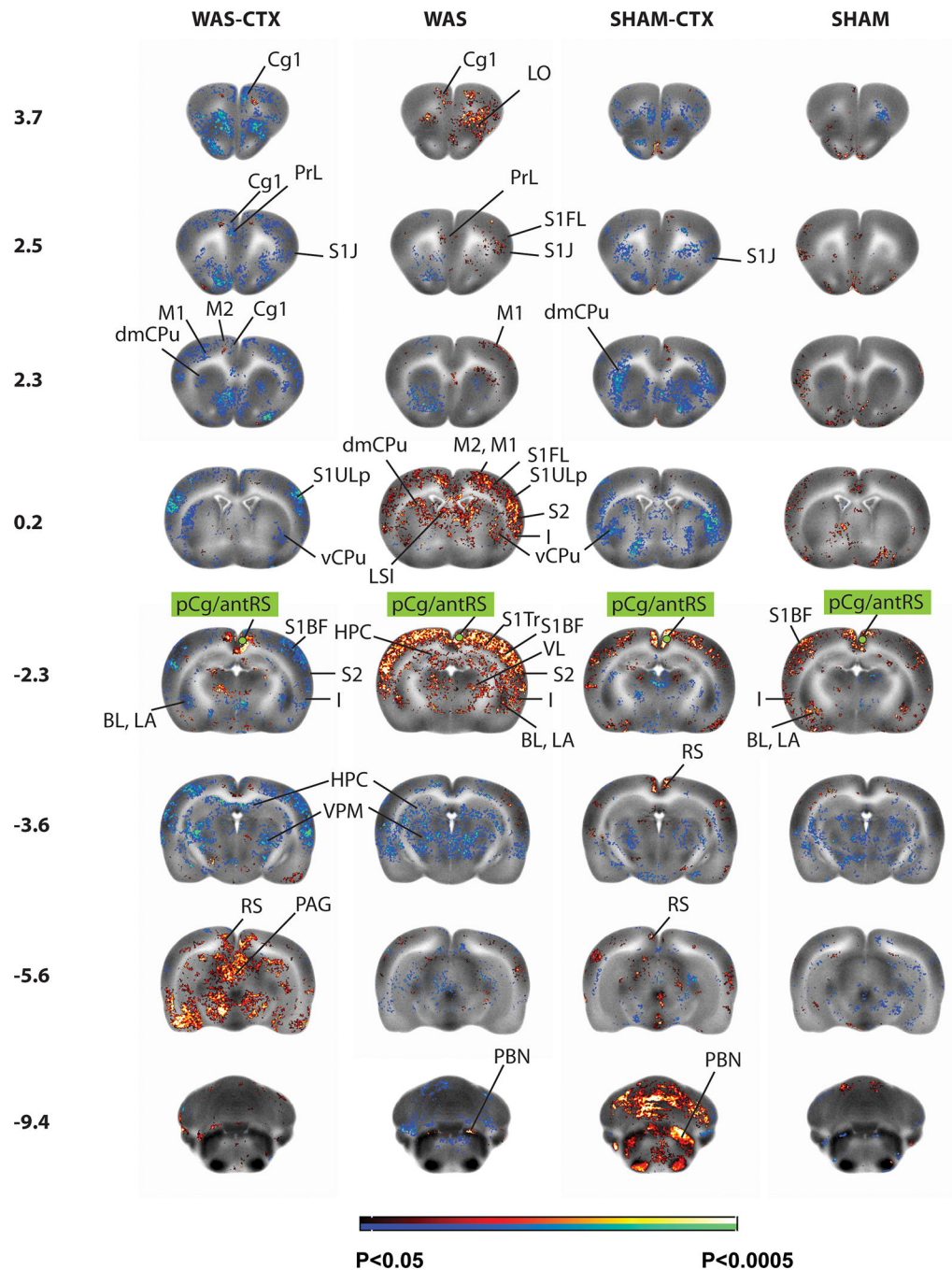


Figure 4: Correlation of functional activity during bladder filling of the right posterior cingulate cortex (seed region in green) across the whole brain.

Changes in regional functional connectivity are depicted on representative coronal sections (anterior–posterior coordinates relative to the bregma) of the template brain. Color-coded overlays show statistically significant group differences, with red and blue colors showing positive and negative functional connectivity, respectively ($P < 0.05$ at the voxel level for clusters of >100 contiguous voxels). Abbreviations are as in figure 2 above.

Table 1:

Significant main effects of ‘Stress’ and ‘Ceftriaxone’ (CTX) and their interaction (ANOVA, Left/Right hemispheres, *P<0.05 for >100 contiguous voxels). Highlighted regions have been proposed to be within the micturition circuit (Fig. 3) ^{128, 129}.

	Stress	CTX	Stress × CTX
CORTEX			
Cingulate			
anterior	* / *	* / *	
mid		* / *	
posterior	* / *	* / *	* / *
Entorhinal, caudomedial	/ *	* / *	* / *
Insula, posterior	* / *	* / *	
Motor, primary		* /	
Motor, secondary	* /	* / *	
Olfactory		* / *	
Orbital	* / *	* / *	
Piriform	* / *	* / *	
Prelimbic	* / *	* / *	
Retrosplenial, anterior	* / *		* / *
posterior		* / *	
Somatosensory, primary	* / *	* / *	* / * SITr
secondary		* / *	/ *
Visual, primary, secondary		* / *	
SUBCORTEX			
Accumbens n.		* / *	
Amygdala			
basolateral		* / *	
basomedial, medial	* / *	* / *	* / *
central		* / *	
cortical	* / *	* / *	
lateral/basolateral		* / *	
Cerebellum, simple lobule	* / *	* / *	* / *
vermis		* / *	
Colliculus, inferior		* / *	
Diagonal band		* / *	
Hippocampus, dorsal anterior	* / *	* / *	
dorsal posterior		* / *	
Hypothalamus			
anterior	* / *	* / *	
posterior	* / *		* / *
preoptic area		* / *	
ventromedial	* / *	* / *	* / *

	Stress	CTX	Stress × CTX
Lateral septum		* / *	
Locus coeruleus		* / *	
Mesencephalic/tegmental area		* / *	
Parabrachial/Barrington nuclear complex		* / *	
Periaqueductal gray, periventricular gray	* / *	* / *	
Postsubiculum		* / *	
Raphe		* / *	
Retrorubral field		* / *	
Septohippocampal n.		* / *	
Striatum			
dorsal		* / *	
dorsomedial		* / *	
lateral		* / *	
ventral, anterior	* /	* /	
Superior olive		* / *	
Thalamus			
anterior medial n., anterior ventral n.	* / *	* / *	* / *
lateral dorsal n.	* / *		* / *
mediodorsal n.	/ *	* / *	/ *
medial geniculate n.		* / *	
paraventricular n.	*	*	
ventral posterolateral n.		* / *	
ventral posteromedial n.		* / *	
ventrolateral n., ventromedial n.		* / *	
Ventral pallidum		* / *	